nature

https://doi.org/10.1038/s41586-020-2058-6

Supplementary information

# Observation of the Kondo screening cloud

In the format provided by the authors and unedited

Ivan V. Borzenets✉, Jeongmin Shim, Jason C. H. Chen, Arne Ludwig, Andreas D. Wieck, Seigo Tarucha, H.-S. Sim✉ & Michihisa Yamamoto✉

# Supplementary Information: Observation of the Kondo screening cloud

I. V. Borzenets[1,6*], J. Shim[2,6], J. Chen[3], A. Ludwig[4], A. Wieck[4], S. Tarucha[5], H.-S. Sim[2*], and M. Yamamoto[5*]

[1]*Department of Physics, City University of Hong Kong, Kowloon Tong, Kowloon, Hong Kong* [2]*Department of Physics, Korea Advanced Institute of Science and Technology (KAIST), Daejeon 34141, South Korea* [3]*Department of Applied Physics, University of Tokyo, Bunkyo-ku, Tokyo, Japan* [4]*Faculty of Physics and Astronomy, Rurh-University Bochum, Bochum, Germany* [5]*Center for Emergent Matter Science (CEMS), RIKEN, Wako-shi, Saitama, Japan* [6]*These authors contributed equally: I. V. Borzenets, J. Shim* [*]*Correspondence should be sent to I.V.B. (email: iborzene@cityu.edu.hk), H.-S.S (email: hssim@kaist.ac.kr), and M.Y. (email: michihisa.yamamoto@riken.jp)*

## I. THEORETICAL MODEL

The essential features of the experimental data are in good agreement with the numerical renormalization group (NRG) calculation of a model described below.

### A. Model Hamiltonian

The experimental setup can be described by theoretical model based on Hamiltonian $H$,

$$H = H_{\mathrm{QD}} + H_{\mathrm{l}} + H_{\mathrm{r}} + H_{\mathrm{tun}}. \tag{S1}$$

In the model, the quantum dot (QD) is described by an Anderson impurity, $H_{\mathrm{QD}} = \sum_{\sigma=\uparrow,\downarrow} \epsilon_{\mathrm{QD}} d_\sigma^\dagger d_\sigma + U d_\uparrow^\dagger d_\uparrow d_\downarrow^\dagger d_\downarrow$, where $d_\sigma^\dagger$ is the operator creating an electron with spin $\sigma$ in the QD, $\epsilon_{\mathrm{QD}}$ is the onsite energy of the electron, and $U$ is the charging energy. The QD couples with the two wires by electron tunneling. The tunneling Hamiltonian is $H_{\mathrm{tun}} = \sum_{w=\mathrm{l,r}} \sum_{\sigma=\uparrow,\downarrow} t_w c_{w1\sigma}^\dagger d_\sigma + \text{h.c.}$, where $t_w$ is the tunneling amplitude between the QD and the first site $j = 1$ of the wire $w = \mathrm{l}, \mathrm{r}$, $c_{wj\sigma}^\dagger$ is the operator creating an electron with spin $\sigma$ in the site $j$ of the wire $w$, and h.c. stands for hermitian conjugate. The left wire is described by a semi-infinite tight-binding chain, $H_{\mathrm{l}} = -\sum_{\sigma=\uparrow,\downarrow} \sum_{j=1}^{\infty} t c_{\mathrm{l}j\sigma}^\dagger c_{\mathrm{l}(j+1)\sigma} + \text{h.c.}$ $t$ is the electron hopping amplitude between neighboring sites of the wire. The right wire is also described by a semi-infinite chain,

$$\begin{aligned} H_{\mathrm{r}} = -\sum_{\sigma=\uparrow,\downarrow} [\sum_{j=1}^{L-1} t c_{\mathrm{r}j\sigma}^\dagger c_{\mathrm{r}(j+1)\sigma} + \sum_{j=L+1}^{\infty} t c_{\mathrm{r}j\sigma}^\dagger c_{\mathrm{r}(j+1)\sigma} \\ + t_0 c_{\mathrm{r}L\sigma}^\dagger c_{\mathrm{r}(L+1)\sigma} + \text{h.c.}]. \end{aligned} \tag{S2}$$

In the right wire, the electron hopping amplitude $t_0$ between the sites $j = L$ and $j = L + 1$ is smaller than the hopping amplitude $t$ of the other part. This describes the effect of the quantum point contact (QPC) formed by $V_{\mathrm{QPC}}$ in the right wire in the experimental setup. As a result, the FP resonant cavity is formed between the first site $j = 1$ and the site $j = L$.

### B. Fabry-Perot resonant cavity

The hybridization function $\Gamma_{\mathrm{r}}$ between the right wire and the QD depends on whether a resonant level of the FP cavity is aligned with the Fermi level [1]. When the Fermi level

$\epsilon_{\mathrm{F}}$ is located at the center of the energy band (i.e., $\epsilon_{\mathrm{F}} = 0$), we compute $\Gamma_{\mathrm{r}}(E)$ at energy $E$ near the Fermi level, using the Hamiltonian in Eq. (S1),

$$\Gamma_{\mathrm{r}}(E) \approx \frac{\Gamma_{\mathrm{r}\infty}}{(1-\alpha)\cos^2(\frac{\pi E}{\Delta} + k_{\mathrm{F}}L) + \frac{1}{1-\alpha}\sin^2(\frac{\pi E}{\Delta} + k_{\mathrm{F}}L)}. \tag{S3}$$

$\Gamma_{\mathrm{r}\infty} = \frac{t_{\mathrm{r}}^2}{2t^2}\sqrt{4t^2 - E^2}$ is the hybridization function in the absence of the QPC (i.e., in the case of $t_0 = t$), $\Delta = \pi\hbar v_{\mathrm{F}}/L$ is the resonance level spacing of the cavity, and $v_{\mathrm{F}}$ is the Fermi velocity. $\alpha = 1 - (t_0/t)^2 \in [0, 1]$ parameterizes the energy broadening of the resonance level by the QPC; larger broadening occurs for smaller $\alpha$. $k_{\mathrm{F}}L$ describes the resonance condition at the Fermi wavevector $k_{\mathrm{F}}$. In the situation of on-resonance (when the center of a resonance level is aligned with the Fermi level), $e^{2ik_{\mathrm{F}}L} = 1$. In the off-resonance case, $e^{2ik_{\mathrm{F}}L} = -1$.

On the other hand, the left wire does not have a FP cavity. The hybridization function $\Gamma_{\mathrm{l}}$ between the left wire and the QD is found as $\Gamma_{\mathrm{l}}(E) = \frac{t_{\mathrm{l}}^2}{2t^2}\sqrt{4t^2 - E^2}$.

### C. Parameter estimation

We estimate the parameters of the model from the experimental data. The estimation is shown in Table S1.

| parameter | value |
|---|---|
| $U$ | 600 $\mu$eV |
| $\epsilon_{\mathrm{QD}}$ | - 300 $\mu$eV ($= -U/2$) |
| $t_{\mathrm{l}}$ | 150 $\mu$eV |
| $t_{\mathrm{r}}$ | 547.5 $\mu$eV to 600 $\mu$eV (3.65$t_{\mathrm{l}}$ to 4$t_{\mathrm{l}}$) |
| $t$ | 3 meV |
| $\Delta$ | 300 $\mu$eV, 120 $\mu$eV, 75 $\mu$eV |
| $\alpha$ | 0.1 |
| $t_0$ | 2.85 meV |
| $T$ | 0.13 K to 0.5 K |

TABLE S1: Parameter estimation used in the analysis.

The QD charging energy $U$ is chosen as 600 $\mu$eV, based on the observed Coulomb diamond. The QD onsite energy is chosen as $\epsilon_{\rm QD} = -U/2$, since the QD is in the Kondo valley in the experiment. The estimated values of the tunneling amplitudes $t_{\rm l}$ and $t_{\rm r}$ agree with the experimental regime of $t_{\rm l} \ll t_{\rm r}$, and with the observed QD conductance ranging from 0.4 $e^2/h$ to 0.6 $e^2/h$. Following the experiment, $t_{\rm l}$ is fixed and $t_{\rm r}$ is tuned in the theoretical analysis. The hopping energy $t$ of the wires is sufficiently larger than the other energy scales. The resonance level spacing $\Delta$ is estimated, based on the observed resonant conductance peaks. We obtain three different values of $\Delta$, corresponding to the three cavity lengths $L$ of the experiment. The resonance level broadening parameter $\alpha \in [0, 1]$ is chosen as $\alpha = 0.1$ with which the experimental data are well described by the model in Eq. (S1). The small value of $\alpha = 0.1$ agrees with the experimental situation that the QPC gate voltage is weak (hence the resonant conductance peaks have wide width). The energy $t_0$, which is the hopping energy between the sites $j = L$ and $j = L + 1$ in the right wire, is determined by the parameters $t$ and $\alpha$ from the relationship $\alpha = 1 - (t_0/t)^2$, as discussed before. Note that $t_0$ is smaller than $t$ due to the QPC gate.

### D. NRG calculation

Using the Hamiltonian in Eq. (S1) and the NRG [2, 3], we compute the conductance $G$ between the left and right wires of the experimental setup. In the computation, the NRG discretization parameter is $\Lambda = 2$, 500 states are kept at each iteration, and $z$-averaging is done for $z = 0, 1/n_z, 2/n_z, \ldots, (n_z - 1)/n_z$ with $n_z = 8$.

Using the NRG result of the QD spectral function $A_{{\rm QD}\sigma}(E, T)$ of spin $\sigma$ at energy $E$, we compute the temperature $T$ dependence of the conductance [4, 5],

$$G(T) = \frac{e^2}{h} \sum_{\sigma=\uparrow,\downarrow} \int dE \left(-\frac{\partial f}{\partial E}\right) \frac{4\pi\Gamma_{\rm l}\Gamma_{\rm r}}{\Gamma_{\rm l} + \Gamma_{\rm r}} A_{{\rm QD}\sigma}, \tag{S4}$$

where $f$ is the Fermi-Dirac distribution.

To compare the experimental data with the NRG result in Fig.3 of the main text, we apply the same method for the estimation of the Kondo temperature to the experimental data and to the NRG result. The method is the fitting to the empirical formula [6]

$$G(T) = G_0\left(\frac{T_{\rm K}^{'2}}{T^2 + T_{\rm K}^{'2}}\right)^s, \qquad T_{\rm K}^{'} = T_{\rm K}\frac{1}{\sqrt{2^{1/s} - 1}} \tag{S5}$$

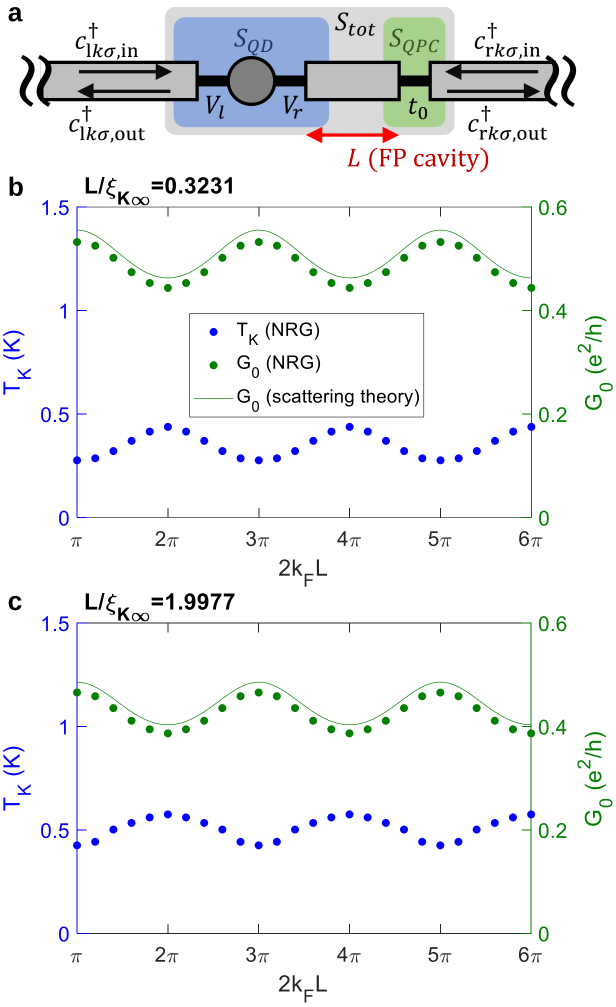


FIG. S1: a) Schematic view for scattering matrices. b-c) The oscillations of the zero-temperature conductance $G_0$ and the Kondo temperature $T_\mathrm{K}$ as a function of $2k_\mathrm{F}L$ for (b) $L/\xi_{\mathrm{K}\infty} = 0.3231$ and (c) 1.9977. The two oscillations are out of phase by $\pi$ in both the cases of $L/\xi_{\mathrm{K}\infty}$. $G_0$ is obtained by using the scattering theory in Eq. (S11) (see blue solid curves) and also by the NRG calculation (blue circles), while $T_\mathrm{K}$ is obtained by applying the empirical formula to the temperature window of [0 K, 0.5 K].

in the temperature window from $T = 0.13$ K to 0.5 K (the window available in the experiment). Here $G_0$ is the zero temperature conductance and $s \approx 0.2$ is a fit parameter. The applicability of the empirical formula to our case of the QD coupled to the FP cavity is discussed in Methods.

## II. CONDUCTANCE OSCILLATION

To explain the conductance oscillation in Fig. 2 of the main text, we construct a scattering theory based on the Fermi liquid theory. The result of the scattering theory agrees with the experimental data and the NRG result.

### A. Scattering theory

We compute the scattering matrix $S_{\mathrm{tot}}$ of the region combining the QD, the FP cavity, and the QPC,

$$\begin{bmatrix} c^{\dagger}_{\mathrm{l}k\sigma,\mathrm{out}} \\ c^{\dagger}_{\mathrm{r}k\sigma,\mathrm{out}} \end{bmatrix} = S_{\mathrm{tot}} \begin{bmatrix} c^{\dagger}_{\mathrm{l}k\sigma,\mathrm{in}} \\ c^{\dagger}_{\mathrm{r}k\sigma,\mathrm{in}} \end{bmatrix} = \begin{bmatrix} r_{\mathrm{tot}} & t'_{\mathrm{tot}} \\ t_{\mathrm{tot}} & r'_{\mathrm{tot}} \end{bmatrix} \begin{bmatrix} c^{\dagger}_{\mathrm{l}k\sigma,\mathrm{in}} \\ c^{\dagger}_{\mathrm{r}k\sigma,\mathrm{in}} \end{bmatrix}, \tag{S6}$$

where $c^{\dagger}_{wk\sigma,\mathrm{in(out)}}$ creates an electron with momentum $k$ and spin $\sigma$ incoming from the wire $w$ to the scattering region (outgoing from the scattering region to the wire $w$). See Fig. S1a. The scattering matrix formalism is applicable to the low-temperature Fermi-liquid regimes. At zero temperature, the electron conductance $G$ between the left and right wires is written as $G(T=0) = G_0 = 2e^2|t_{\mathrm{tot}}|^2/h$ [5].

$S_{\mathrm{tot}}$ is obtained by combining the scattering matrix $S_{\mathrm{QD}}$ of the QD, the scattering matrix $S_{\mathrm{QPC}}$ of the QPC, and the dynamical phase gain of plane waves propagating through the FP cavity. By using the equation of motions for Green function and the Fermi liquid theory [4, 5], $S_{\mathrm{QD}}$ and $S_{\mathrm{QPC}}$ are obtained as

$$S_{\mathrm{QD}} = \frac{1}{t_{\mathrm{l}}^2 + t_{\mathrm{r}}^2} \begin{bmatrix} e^{2i\delta} t_{\mathrm{l}}^2 + t_{\mathrm{r}}^2 & (e^{2i\delta} - 1) t_{\mathrm{l}} t_{\mathrm{r}} \\ (e^{2i\delta} - 1) t_{\mathrm{l}} t_{\mathrm{r}} & t_{\mathrm{l}}^2 + e^{2i\delta} t_{\mathrm{r}}^2 \end{bmatrix}, \tag{S7}$$

$$S_{\mathrm{QPC}} = \frac{1}{2-\alpha} \begin{bmatrix} \alpha & 2i\sqrt{1-\alpha} \\ 2i\sqrt{1-\alpha} & \alpha \end{bmatrix}. \tag{S8}$$

Here $\delta$ is the scattering phase shift by the QD, and $\delta = \pi/2$ at zero temperature in the Kondo regime. $S_{\mathrm{tot}}$ can be obtained from

$$M_{\mathrm{tot}} = M_{\mathrm{QPC}} \begin{bmatrix} e^{ikL} & \\ & e^{-ikL} \end{bmatrix} M_{\mathrm{QD}}. \tag{S9}$$

Here $e^{ikL}$ is the dynamical phase gain of an electron with momentum $k$ propagating through the FP cavity, and the matrices $M$'s are the transfer matrices related with the corresponding scattering matrix via

$$S_a = \begin{bmatrix} s_{11} & s_{12} \\ s_{21} & s_{22} \end{bmatrix} \leftrightarrow M_a = \frac{1}{s_{22}} \begin{bmatrix} s_{12}s_{21} - s_{11}s_{22} & s_{22} \\ -s_{11} & 1 \end{bmatrix}, \tag{S10}$$

for $a = \text{tot}, \text{QD}, \text{QPC}$. We find that the transmission amplitude $t_{\text{tot}}$ through the whole scattering region containing the QD and the FP cavity is written as

$$t_{\text{tot}} = \frac{-2i\sqrt{1-\alpha}(e^{2i\delta}-1)t_{\text{l}}t_{\text{r}}e^{ik_{\text{F}}L}}{[2-(1+e^{2ik_{\text{F}}L})\alpha]t_{\text{l}}^2 + [2-(1+e^{2i\delta}e^{2ik_{\text{F}}L})\alpha]t_{\text{r}}^2} \tag{S11}$$

for electrons at the Fermi level.

### B. The Kondo regime

We apply the scattering-theory result in Eq. (S11) to the case that the QD is in the Kondo regime. In this case, the scattering phase shift $\delta = \pi/2$ at zero temperature, according to the Fermi liquid theory. Using the estimated parameters in Table S1, we compute the zero-temperature conductance $G_0 = 2e^2|t_{\text{tot}}|^2/h$. As shown in Fig. S1, the conductance $G_0$ obtained by using the scattering theory is in good agreement with the conductance obtained by the NRG formula in Eq. (S4). Interestingly, the conductance exhibits the maximum value at the off-resonance conditions of $e^{2ik_{\text{F}}L} = -1$, and shows the minimum value at the on-resonance conditions of $e^{2ik_{\text{F}}L} = 1$. This results from the phase shift $\delta = \pi/2$. On the other hand, the Kondo temperature has the maximum (minimum) value at the on-resonance (off-resonance) conditions; note that the same conclusion is obtained when the Kondo temperature is estimated by using $T_{\text{K}} = \exp(-\pi U/8\Gamma)$ and $\Gamma = \Gamma_{\text{l}}(E=\epsilon_{\text{F}}) + \Gamma_{\text{r}}(E=\epsilon_{\text{F}})$. Therefore, the oscillations of $G_0$ and $T_{\text{K}}$ as a function of $2k_{\text{F}}L$ are out of phase by $\pi$. This out-of-phase behavior occurs in both the regimes of $L/\xi_{\text{K}\infty} > 1$ and $L/\xi_{\text{K}\infty} < 1$, and at low temperature $T \lesssim T_{\text{K}}, \Delta$. This agrees with the experimental data in Fig. 2.

### C. A single noninteracting level

We note that the out-of-phase behavior of the oscillations of $G_0$ and $T_{\text{K}}$ occurs also in the case that the QD effectively has only a single noninteracting level at the Fermi level. It is because the QD energy level aligned with the Fermi level results in the scattering phase shift $\delta = \pi/2$ as in the Kondo regime. This argument is applicable to the case that the QD shows Coulomb blockade resonance, and it agrees with our experimental data.

## III. COMPATIBILITY WITH NRG CALCULATIONS

### A. Estimating $T_{\mathrm{K}}$

The estimation of the Kondo temperature $T_{\mathrm{K}}$ based on the empirical formula works well when the hybridization functions of the reservoirs coupled to the QD are energy independent near the Fermi level over the energy scale much larger than Kondo temperature. In our experiment, however, the hybridization function $\Gamma_{\mathrm{r}}$ of the right wire is energy dependent, because of the resonances formed in the FP cavity. Below we show, based on the NRG calculation, that the empirical formula is still useful for estimating $T_{\mathrm{K}}$ in our experiment regime of $L \lesssim \xi_{\mathrm{K}\infty}$.

Figure S2a shows the NRG result of the temperature dependence of the conductance in a case of $L \lesssim \xi_{\mathrm{K}\infty}$. In this case, the resonance level spacing $\Delta$ of the FP cavity is larger than Kondo temperature $T_{\mathrm{K}\infty}$, hence, the hybridization function $\Gamma_r$ is almost energy independent near the Fermi level (see the inset of Fig. S2a) both in the situations of on- and off-resonance; the zero-temperature conductance at on-resonance is smaller than that at off-resonance due to the phase shift $\delta = \pi/2$ as discussed in Sec. II B. We notice that the NRG result is well fitted to the empirical formula in this case, although the NRG result slightly deviate from the empirical formula around the temperature comparable to the resonance level spacing $\Delta$. When $L \gtrsim \xi_{\mathrm{K}\infty}$, the deviation could result in an error in estimating the Kondo temperature (see, e.g., a bump in the NRG data of Fig. 3 around $L = 0.6\xi_{\mathrm{K}\infty}$). However, this error does not exceed the experimental error of the Kondo temperature about 20%.

The deviation becomes pronounced in the opposite regime of $L \gg \xi_{\mathrm{K}\infty}$ (note that our experiment is not in this regime). In this regime, there are many resonances within the energy window of $T_{\mathrm{K}\infty}$ near the Fermi level, as shown in the inset of Fig. S2b. As a result, the conductance has unusual temperature dependence at temperature comparable to the resonance level spacing $\Delta$, hence, the empirical formula does not well describe the temperature dependence. For example, at on-resonance, the conductance is almost constant near

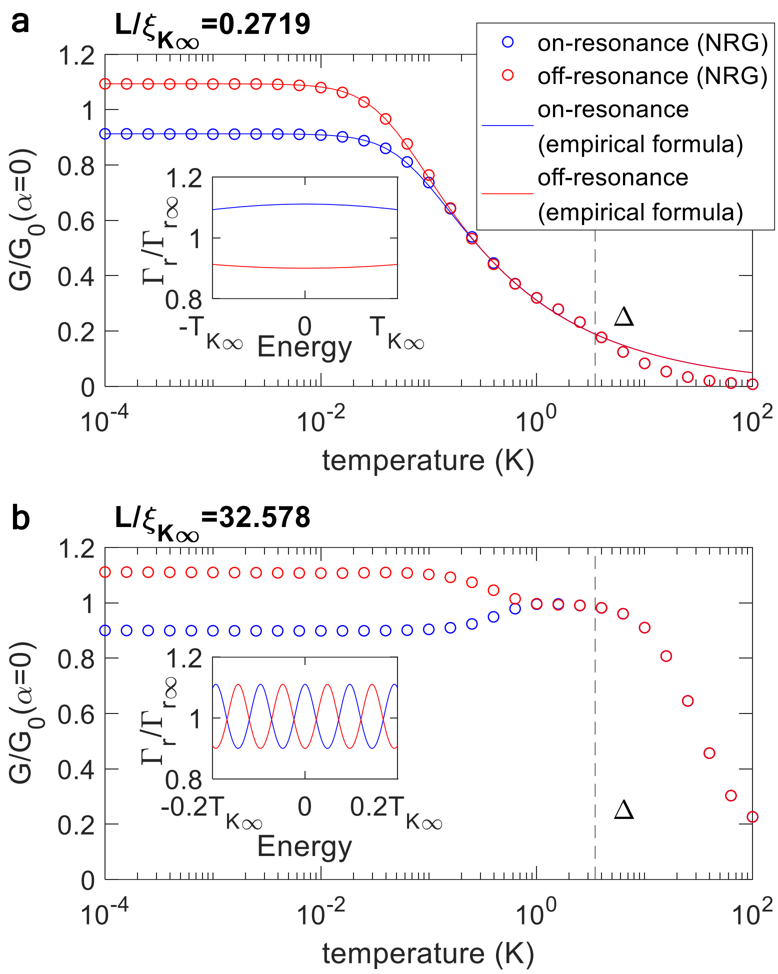


FIG. S2: NRG results of the conductance $G$ as a function of temperature $T$ at on-resonance (blue circles) and off-resonance (red) in the cases of (a) $L < \xi_{\mathrm{K}\infty}$ and (b) $L > \xi_{\mathrm{K}\infty}$. In (a), the NRG results in the temperature window of [0 K, 0.5 K] are well fitted to the empirical formula (see solid curves). The vertical dashed lines indicate the temperature comparable to the resonance level spacing $\Delta$. Inset: The hybridization function $\Gamma_{\mathrm{r}}$ as a function of energy $E$ at on-resonance (blue curve) and off-resonance (red).

$T = 0$, increases slowly with temperature at $T \lesssim \Delta$, and then decreases at $T \gtrsim \Delta$. This is because the conductance is governed by a single resonance near $T = 0$, and then by multiple resonances near $T \sim \Delta$. We note that similar but stronger deviation can occur in the regime of a Kondo box [7–9].

We note that the energy-dependent hybridization due to the resonances can be well described by the NRG, especially in the regime of our manuscript where a weak barrier is applied to form the FP cavity. The NRG shows a few percent (or less) error in computing conductance due to the discretization for the case of a constant hybridization function. We have checked that the same order of error is found for the energy-dependent hybridization of the regime of our manuscript. The same order of error can be understood from the fact that a weak oscillation of the density of states of conduction electrons near the Kondo impurity site affects the hybridization in a linear energy scale, while the discretization treats the hybridization in a logarithmic energy scale. The NRG calculation has been applied to cases of an energy-dependent hybridization [1, 9–11]; In Ref. [9], the NRG has been applied even to a Kondo box where the hybridization has rather strong energy dependence.

### B. Estimating $T_{\mathrm{K}\infty}$

In the experiment, $T_{\mathrm{K}\infty}$, the Kondo temperature of the case where no QPC is formed in the right wire, cannot be directly obtained, since the QPC gate affects the right wire even when the gate voltage $V_{\mathrm{QPC}}$ is turned off. We estimate it as $T_{\mathrm{K}\infty} \approx \sqrt{T_{\mathrm{K,Max}} T_{\mathrm{K,Min}}}$, the geometric mean of $T_{\mathrm{K,Max}}$ and $T_{\mathrm{K,Min}}$, where $T_{\mathrm{K,Max}}$ ($T_{\mathrm{K,Min}}$) is the maximum (minimum) value of $T_{\mathrm{K}}$ among those obtained with tuning $2k_{\mathrm{F}}L$ in the experiment.

In Fig. S3 we compare $T_{\mathrm{K}\infty}$ and $\sqrt{T_{\mathrm{K,Max}} T_{\mathrm{K,Min}}}$, which we compute by using the NRG, the Hamiltonian in Eq. (S1) and the parameters in Table S1. This shows that the estimation of $T_{\mathrm{K}\infty}$ from the experimental data of $\sqrt{T_{\mathrm{K,Max}} T_{\mathrm{K,Min}}}$ is valid.

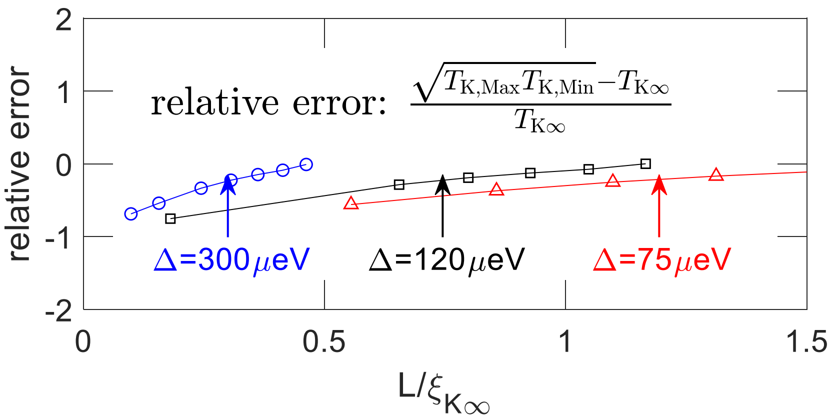


FIG. S3: Comparison between $T_{\mathrm{K}\infty}$ and $\sqrt{T_{\mathrm{K,Max}} T_{\mathrm{K,Min}}}$, which are obtained by using the NRG method.

We expect such good agreement between $T_{\mathrm{K}\infty}$ and $\sqrt{T_{\mathrm{K,Max}} T_{\mathrm{K,Min}}}$ in our experimental regime of $t_{\mathrm{l}} \ll t_{\mathrm{r}}$, $\Delta \gtrsim T_{\mathrm{K}\infty}$, and small $\alpha$ satisfying $(1-\alpha)^{-1} \approx 1 + \alpha$. In this regime, we find $T_{\mathrm{K,Max}} \approx (T_{\mathrm{K}\infty})^{1-\alpha}$ and $T_{\mathrm{K,Min}} \approx (T_{\mathrm{K}\infty})^{1+\alpha}$, by using the expression [4] of $T_{\mathrm{K}\infty} \sim \exp(-\frac{\pi U}{8\Gamma_{r\infty}(E=\epsilon_{\mathrm{F}})})$ at the on- and off-resonances of $e^{2ik_{\mathrm{F}}L} = \pm 1$. This provides $T_{\mathrm{K}\infty} \approx \sqrt{T_{\mathrm{K,Max}} T_{\mathrm{K,Min}}}$.

## IV. KONDO PEAK VERSUS BIAS

It is expected that in addition to the trend of conductance versus device temperature, the effect of Kondo Temperature will also manifest itself in Kondo peak conductance versus bias voltage $V_{\mathrm{SD}}$. That is, the conductance associated with the Kondo effect will be highest at zero bias, and decay with increased $|V_{\mathrm{SD}}|$, with the width of this "zero bias peak" following $T_{\mathrm{K}}$[12]. In Figure S4 we present measurements of conductance versus bias $V_{\mathrm{SD}}$ and QPC voltage $V_{\mathrm{QPC}}$. Note, that this data was collected as part of an early set of measurements on the device, and we can not directly compare it to any dataset used for the main text. Additionally, this zero bias peak suffers from the background current that increases with $V_{\mathrm{SD}}$ (Figure S4c). While we extracted full width at half maximum (FHMW) by subtraction

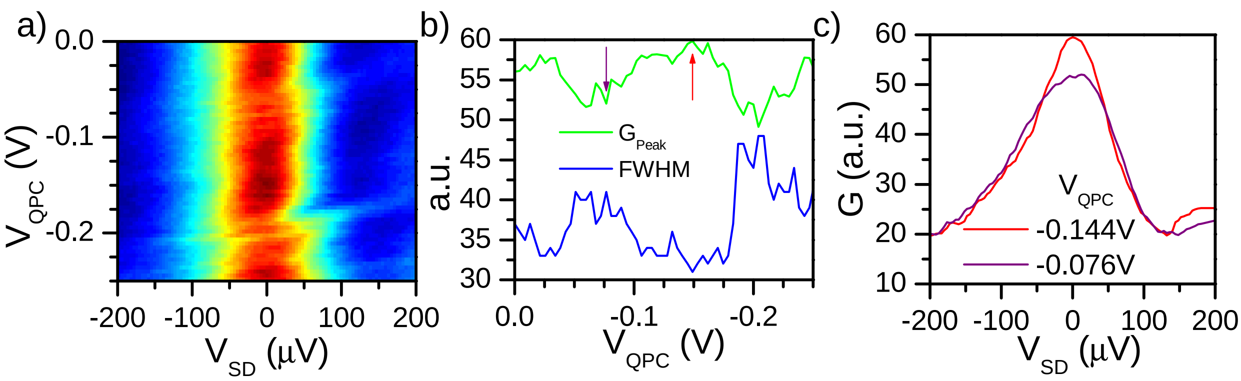


FIG. S4: a)Map of conductance of the Kondo valley center versus bias voltage $V_{\mathrm{SD}}$ and QPC voltage $V_{\mathrm{QPC}}$. The data was taken in an earlier measurement which was not included in the main text. b)The peak conductance $G_{\mathrm{Peak}}$ at $V_{\mathrm{SD}} = 0$ (green) , and width (blue) of the Kondo peak (with respect to $V_{\mathrm{SD}}$) versus $V_{\mathrm{QPC}}$. Note that the width which is expected to follow $T_{\mathrm{K}}$ is out of phase with conductance. c) Line cuts from panel (a) showing conductrance $G$ versus bias voltage $V_{\mathrm{SD}}$. The red curve presents conductance at QPC voltage $V_{\mathrm{QPC}}$ that corresponds to the F-P oscillation peak, while the purple curve is taken at $V_{\mathrm{QPC}}$ corresponding to the dip. Here it is clear that the lower peak is indeed wider.

of a constant background, this FHMW value is not directly proportional to the Kondo temperature. Even though we are unable to quantitatively extract a Kondo temperature from conductance vs $V_{\mathrm{SD}}$ data, qualitatively, we find that the oscillations in peak width with respect to $V_{\mathrm{QPC}}$ are anti-phase with conductance similar to the behavior of $T_{\mathrm{K}}$.

---


[1] J. Park, S.-S. B. Lee, Y. Oreg, and H.-S. Sim, *How to Directly Measure a Kondo Cloud's Length*, Phys. Rev. Lett. **110**, 246603 (2013).

[2] K. G. Wilson, *The renormalization group: Critical phenomena and the Kondo problem*, Rev. Mod. Phys. **47**, 773 (1975).

[3] R. Bulla, T. A. Costi, and T. Pruschke, *Numerical renormalization group method for quantum impurity systems*, Rev. Mod. Phys. **80**, 395 (2008).

[4] A. C. Hewson, *The Kondo Problem to Heavy Fermions* (Cambridge University Press, Cambridge, England, 1993).

[5] M. Pustilnik and L. Glazman, *Kondo effect in quantum dots*, J. Phys. Condens. Matter **16**, R512 (2004).

[6] D. Goldhaber-Gordon, J. Göres, M. A. Kastner, Hadas Shtrikman, D. Mahalu, and U. Meirav, *From the Kondo Regime to the Mixed-Valence Regime in a Single-Electron Transistor*, Phys. Rev. Lett. **81**, 5225 (1998).

[7] W. B. Thimm, J. Kroha, and J. von Delft, *Kondo Box: A Magnetic Impurity in an Ultrasmall Metallic Grain*, Phys. Rev. Lett. **82**, 2143 (1999).

[8] P. Simon and I. Affleck, *Finite-Size Effects in Conductance Measurements on Quantum Dots*, Phys. Rev. Lett. **89**, 206602 (2002).

[9] P. S. Cornaglia and C. A. Balseiro, *Transport through Quantum Dots in Mesoscopic Circuits*, Phys. Rev. Lett. **90**, 216801 (2003).

[10] L. Borda, *Kondo screening cloud in a one-dimensional wire: Numerical renormalization group study*, Phys. Rev. B **75**, 041307 (2007).

[11] G. Yoo, S.-S. B. Lee, and H.-S. Sim, *Detecting Kondo Entanglement by Electron Conductance*, Phys. Rev. Lett. **120**, 146801 (2018).

[12] W. G. van der Wiel, S. De Franceschi, T. Fujisawa, J. M. Elzerman, S. Tarucha, L. P. Kouwenhoven, *The Kondo Effect in the Unitary Limit*, Science, **289**, 5487, pp. 2105-2018 (2000).